

$\psi(2S)$ Decays into J/ψ plus Two Photons

J. Z. Bai¹, Y. Ban¹⁰, J. G. Bian¹, X. Cai¹, J. F. Chang¹, H. F. Chen¹⁶, H. S. Chen¹, H. X. Chen¹, J. Chen¹, J. C. Chen¹, Jun Chen⁶, M. L. Chen¹, Y. B. Chen¹, S. P. Chi², Y. P. Chu¹, X. Z. Cui¹, H. L. Dai¹, Y. S. Dai¹⁸, Z. Y. Deng¹, L. Y. Dong¹, S. X. Du¹, Z. Z. Du¹, J. Fang¹, S. S. Fang², C. D. Fu¹, H. Y. Fu¹, L. P. Fu⁶, C. S. Gao¹, M. L. Gao¹, Y. N. Gao¹⁴, M. Y. Gong¹, W. X. Gong¹, S. D. Gu¹, Y. N. Guo¹, Y. Q. Guo¹, Z. J. Guo¹⁵, S. W. Han¹, F. A. Harris¹⁵, J. He¹, K. L. He¹, M. He¹¹, X. He¹, Y. K. Heng¹, H. M. Hu¹, T. Hu¹, G. S. Huang¹, L. Huang⁶, X. P. Huang¹, X. B. Ji¹, Q. Y. Jia¹⁰, C. H. Jiang¹, X. S. Jiang¹, D. P. Jin¹, S. Jin¹, Y. Jin¹, Y. F. Lai¹, F. Li¹, G. Li¹, H. H. Li¹, J. Li¹, J. C. Li¹, Q. J. Li¹, R. B. Li¹, R. Y. Li¹, S. M. Li¹, W. Li¹, W. G. Li¹, X. L. Li⁷, X. Q. Li⁷, X. S. Li¹⁴, Y. F. Liang¹³, H. B. Liao⁵, C. X. Liu¹, Fang Liu¹⁶, F. Liu⁵, Feng Liu¹, H. M. Liu¹, J. B. Liu¹, J. P. Liu¹⁷, R. G. Liu¹, Y. Liu¹, Z. A. Liu¹, Z. X. Liu¹, G. R. Lu⁴, F. Lu¹, J. G. Lu¹, C. L. Luo⁸, X. L. Luo¹, F. C. Ma⁷, J. M. Ma¹, L. L. Ma¹¹, X. Y. Ma¹, Z. P. Mao¹, X. C. Meng¹, X. H. Mo¹, J. Nie¹, Z. D. Nie¹, S. L. Olsen¹⁵, H. P. Peng¹⁶, N. D. Qi¹, C. D. Qian¹², H. Qin⁸, J. F. Qiu¹, Z. Y. Ren¹, G. Rong¹, L. Y. Shan¹, L. Shang¹, D. L. Shen¹, X. Y. Shen¹, H. Y. Sheng¹, F. Shi¹, X. Shi¹⁰, L. W. Song¹, H. S. Sun¹, S. S. Sun¹⁶, Y. Z. Sun¹, Z. J. Sun¹, X. Tang¹, N. Tao¹⁶, Y. R. Tian¹⁴, G. L. Tong¹, G. S. Varner¹⁵, D. Y. Wang¹, J. Z. Wang¹, L. Wang¹, L. S. Wang¹, M. Wang¹, Meng Wang¹, P. Wang¹, P. L. Wang¹, S. Z. Wang¹, W. F. Wang¹, Y. F. Wang¹, Zhe Wang¹, Z. Wang¹, Zheng Wang¹, Z. Y. Wang¹, C. L. Wei¹, N. Wu¹, Y. M. Wu¹, X. M. Xia¹, X. X. Xie¹, B. Xin⁷, G. F. Xu¹, H. Xu¹, Y. Xu¹, S. T. Xue¹, M. L. Yan¹⁶, W. B. Yan¹, F. Yang⁹, H. X. Yang¹⁴, J. Yang¹⁶, S. D. Yang¹, Y. X. Yang³, L. H. Yi⁶, Z. Y. Yi¹, M. Ye¹, M. H. Ye², Y. X. Ye¹⁶, C. S. Yu¹, G. W. Yu¹, C. Z. Yuan¹, J. M. Yuan¹, Y. Yuan¹, Q. Yue¹, S. L. Zang¹, Y. Zeng⁶, B. X. Zhang¹, B. Y. Zhang¹, C. C. Zhang¹, D. H. Zhang¹, H. Y. Zhang¹, J. Zhang¹, J. M. Zhang⁴, J. Y. Zhang¹, J. W. Zhang¹, L. S. Zhang¹, Q. J. Zhang¹, S. Q. Zhang¹, X. M. Zhang¹, X. Y. Zhang¹¹, Yiyun Zhang¹³, Y. J. Zhang¹⁰, Y. Y. Zhang¹, Z. P. Zhang¹⁶, Z. Q. Zhang⁴, D. X. Zhao¹, J. B. Zhao¹, J. W. Zhao¹, P. P. Zhao¹, W. R. Zhao¹, X. J. Zhao¹, Y. B. Zhao¹, Z. G. Zhao^{1*}, H. Q. Zheng¹⁰, J. P. Zheng¹, L. S. Zheng¹, Z. P. Zheng¹, X. C. Zhong¹, B. Q. Zhou¹, G. M. Zhou¹, L. Zhou¹, N. F. Zhou¹, K. J. Zhu¹, Q. M. Zhu¹, Yingchun Zhu¹, Y. C. Zhu¹, Y. S. Zhu¹, Z. A. Zhu¹, B. A. Zhuang¹, B. S. Zou¹.

(BES Collaboration)

¹ Institute of High Energy Physics, Beijing 100039, People's Republic of China

² China Center of Advanced Science and Technology, Beijing 100080, People's Republic of China

³ Guangxi Normal University, Guilin 541004, People's Republic of China

⁴ Henan Normal University, Xinxiang 453002, People's Republic of China

⁵ Huazhong Normal University, Wuhan 430079, People's Republic of China

⁶ Hunan University, Changsha 410082, People's Republic of China

⁷ Liaoning University, Shenyang 110036, People's Republic of China

⁸ Nanjing Normal University, Nanjing 210097, People's Republic of China

⁹ Nankai University, Tianjin 300071, People's Republic of China

¹⁰ Peking University, Beijing 100871, People's Republic of China

¹¹ Shandong University, Jinan 250100, People's Republic of China

¹² Shanghai Jiaotong University, Shanghai 200030, People's Republic of China

¹³ Sichuan University, Chengdu 610064, People's Republic of China

¹⁴ Tsinghua University, Beijing 100084, People's Republic of China

¹⁵ University of Hawaii, Honolulu, Hawaii 96822

¹⁶ University of Science and Technology of China, Hefei 230026, People's Republic of China

¹⁷ Wuhan University, Wuhan 430072, People's Republic of China

¹⁸ Zhejiang University, Hangzhou 310028, People's Republic of China

* Visiting professor to University of Michigan, Ann Arbor, MI 48109 USA

Using $\gamma\gamma J/\psi, J/\psi \rightarrow e^+e^-$ and $\mu^+\mu^-$ events from a sample of 14.0×10^6 $\psi(2S)$ decays collected with the BESII detector, the branching fractions for $\psi(2S) \rightarrow \pi^0 J/\psi$, $\eta J/\psi$, and $\psi(2S) \rightarrow \gamma\chi_{c1}, \gamma\chi_{c2} \rightarrow \gamma\gamma J/\psi$ are measured to be $B(\psi(2S) \rightarrow \pi^0 J/\psi) = (1.43 \pm 0.14 \pm 0.13) \times 10^{-3}$, $B(\psi(2S) \rightarrow \eta J/\psi) = (2.98 \pm 0.09 \pm 0.23)\%$, $B(\psi(2S) \rightarrow \gamma\chi_{c1} \rightarrow \gamma\gamma J/\psi) = (2.81 \pm 0.05 \pm 0.23)\%$, and $B(\psi(2S) \rightarrow \gamma\chi_{c2} \rightarrow \gamma\gamma J/\psi) = (1.62 \pm 0.04 \pm 0.12)\%$.

PACS numbers: 13.20.Gd, 13.25.Gv, 13.40.Hq, 14.40.Gx

I. INTRODUCTION

Experimental data for the processes $\psi(2S) \rightarrow \pi^0 J/\psi$, $\eta J/\psi$, and $\gamma\chi_{c1,2}$ are scarce and were mainly taken in the 1970s and 80s [1–6]. The branching fractions from different experiments do not agree well, and the $\pi^0 J/\psi$ channel is measured with low precision. In particular, improved branching fractions for $\psi(2S) \rightarrow \gamma\chi_{cJ}$ are very important for the measurement of χ_{cJ} decay branching fractions using $\psi(2S)$ data. All these appeal for high statistics measurements of these channels.

In this paper, we report on the analysis of $\psi(2S) \rightarrow \pi^0 J/\psi$, $\eta J/\psi$ and $\gamma\chi_{c1,2}$ decays based on a sample of 14.0×10^6 $\psi(2S)$ events collected with the BESII detector. The first two decays are important to test various theoretical predictions for the ratios $R = \frac{\Gamma(\psi(2S) \rightarrow \pi^0 J/\psi)}{\Gamma(\psi(2S) \rightarrow \eta J/\psi)}$, $R' = \frac{\Gamma(\Upsilon' \rightarrow \eta \Upsilon)}{\Gamma(\psi(2S) \rightarrow \eta J/\psi)}$, and $R'' = \frac{\Gamma(\Upsilon'' \rightarrow \eta \Upsilon)}{\Gamma(\psi(2S) \rightarrow \eta J/\psi)}$. The ratio R has been calculated by different theoretical approaches [7], [8] [9], and the ratios R' and R'' have been predicted in the framework of the QCD multipole expansion mechanism [10] [11].

II. THE BES DETECTOR

The Beijing Spectrometer (BES) detector is a conventional solenoidal magnet detector that is described in detail in Ref. [12]; BESII is the upgraded version of the BES detector [13]. A 12-layer vertex chamber (VC) surrounding the beam pipe provides trigger information. A forty-layer main drift chamber (MDC), located radially outside the VC, provides trajectory and energy loss (dE/dx) information for charged tracks over 85% of the total solid angle. The momentum resolution is $\sigma_p/p = 0.017\sqrt{1+p^2}$ (p in GeV/c), and the dE/dx resolution for hadron tracks is $\sim 8\%$. An array of 48 scintillation counters surrounding the MDC measures the time-of-flight (TOF) of charged tracks with a resolution of ~ 200 ps for hadrons. Radially outside the TOF system is a 12 radiation length, lead-gas barrel shower counter (BSC). This measures the energies of electrons and photons over $\sim 80\%$ of the total solid angle with an energy resolution of $\sigma_E/E = 22\%/\sqrt{E}$ (E in GeV). Outside of the solenoidal coil, which provides a 0.4 Tesla magnetic field over the tracking volume, is an iron flux return that is instrumented with three double layers of counters that identify muons of momentum greater than 0.5 GeV/c.

A GEANT3 based Monte Carlo program with detailed consideration of the detector performance (such as dead electronic channels) is used to simulate the BESII detector. The consistency between data and Monte Carlo has been carefully checked in many high purity physics channels, and the agreement is quite reasonable.

III. EVENT SELECTION

The data sample used for this analysis consists of $(14.00 \pm 0.56) \times 10^6$ $\psi(2S)$ events [14] collected with the BESII detector at the center-of-mass energy $\sqrt{s} = M_{\psi(2S)}$. The channels investigated are $\psi(2S)$ decaying into $(\pi^0, \eta)J/\psi$ and $\gamma\chi_{c1,2}$, with $\chi_{c1,2}$ decaying to $\gamma J/\psi$, π^0 and η to two photons, and J/ψ to lepton pairs. They all have a final $\gamma\gamma l^+ l^-$ ($l = e, \mu$) event topology.

A. General selection for $\gamma\gamma l^+ l^-$ events

A neutral cluster is considered to be a photon candidate if it is located within the BSC fiducial region ($|\cos\theta| < 0.75$), the energy deposited in the BSC is greater than 50 MeV, the first hit appears in the first 6 radiation lengths, the angle between the cluster and the nearest charged track is greater than 14° . Each charged track is required to be well fit by a three-dimensional helix and to have a polar angle, θ , within the fiducial region $|\cos\theta| < 0.8$. To ensure tracks originate from the interaction region, we require $V_{xy} = \sqrt{V_x^2 + V_y^2} < 2$ cm and $|V_z| < 20$ cm, where V_x , V_y , and V_z are the x, y, and z coordinates of the point of closest approach of each track to the beam axis.

Events with two charged tracks and two or three photon candidates are subject to further selection criteria. The two charged tracks are identified as an electron pair or muon pair if $0 < S < 0.6$ or $S > 0.9$, respectively, where

$$S = \sqrt{\left(\frac{E_{sc1}}{p_1} - 1\right)^2 + \left(\frac{E_{sc2}}{p_2} - 1\right)^2}$$

and p and E_{sc} are the momentum and the deposited energy in the BSC of a charged track.

A five constraint (5C) kinematic fit to the hypothesis $\psi(2S) \rightarrow \gamma\gamma l^+ l^-$ with the invariant mass of the lepton pair constrained to the J/ψ mass is performed, and the fit probability is required to be greater than 0.01. For events with three photon candidates, the combination of two photons having the smaller χ^2 is chosen. Fig. 1 shows a scatter plot of the invariant mass of the reconstructed J/ψ and the photon with higher energy ($M_{\gamma h, J/\psi}$) versus the invariant mass of two photons ($M_{\gamma\gamma}$) for the $\gamma\gamma\mu^+\mu^-$ final state. The corresponding plot for the $\gamma\gamma e^+e^-$ state is very similar. The η , χ_{c1} , and χ_{c2} signals are quite prominent, while the π^0 signal is much less so. The corresponding plot for 200,000 Monte Carlo simulated $\psi(2S) \rightarrow \pi^0\pi^0 J/\psi$ events, which is the main background for the studied channels, is shown in Fig. 2.

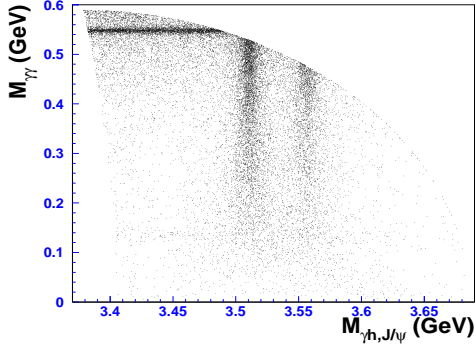


FIG. 1: $M_{\gamma h, J/\psi}$ versus $M_{\gamma\gamma}$ after general selection of $\gamma\gamma\mu^+\mu^-$ events.

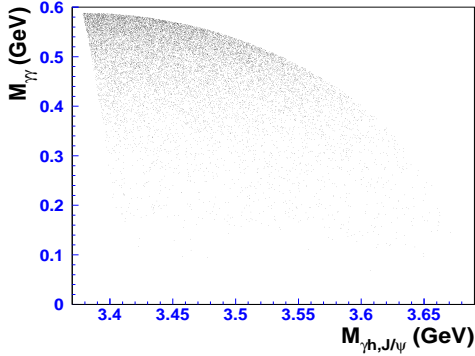


FIG. 2: $M_{\gamma h, J/\psi}$ versus $M_{\gamma\gamma}$ after general selection for 200,000 $\psi(2S) \rightarrow \pi^0\pi^0 J/\psi$ Monte Carlo events ($\gamma\gamma\mu^+\mu^-$ final state).

B. Selection of $\psi(2S) \rightarrow \pi^0 J/\psi$

To remove the huge background from $\psi(2S) \rightarrow \gamma\chi_{c1,c2}$ under the $\psi(2S) \rightarrow \pi^0 J/\psi$ signal, we require $M_{\gamma h, J/\psi}$ to be less than 3.49 or greater than 3.58 GeV/c^2 . Fig. 3 shows, after this requirement, the distribution of invariant mass, $M_{\gamma\gamma}$, where the smooth background is contributed by $\psi(2S) \rightarrow \gamma\chi_{c1,2}$ and $\psi(2S) \rightarrow \pi^0\pi^0 J/\psi$. A Breit Wigner with a double Gaussian mass resolution function to describe the π^0 resonance plus a third-order background polynomial is fitted to the data. The fit gives $N_{e^+e^-}^{\pi^0} = 123 \pm 18$ for the $\gamma\gamma e^+e^-$ state and $N_{\mu^+\mu^-}^{\pi^0} = 155 \pm 20$ for the $\gamma\gamma\mu^+\mu^-$ state. In the fit, the mass resolution and the area ratio of the two Gaussians are fixed to the values determined by the Monte Carlo. The fit is also performed with a background function determined by Monte Carlo simulated $\psi(2S) \rightarrow \pi^0\pi^0 J/\psi$ and $\psi(2S) \rightarrow \gamma\chi_{c1,2}$ events that satisfy the selection criteria, where the two processes are weighted according to their branching fractions. The differences in the number of events obtained with the two backgrounds

(5.1% for $\gamma\gamma e^+e^-$ and 4.3% for $\gamma\gamma\mu^+\mu^-$) are included in the systematic errors.

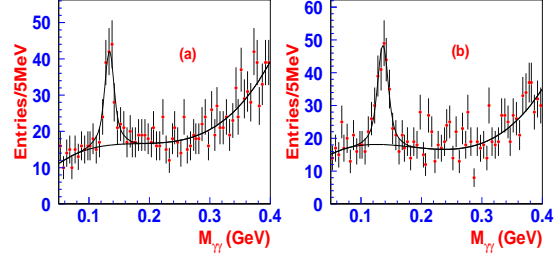


FIG. 3: Two photon invariant mass distribution for candidate $\psi(2S) \rightarrow \pi^0 J/\psi$ events for (a) $\gamma\gamma e^+e^-$ and (b) $\gamma\gamma\mu^+\mu^-$.

C. Selection of $\psi(2S) \rightarrow \eta J/\psi$

In this channel the main backgrounds are from $\psi(2S) \rightarrow \pi^0\pi^0 J/\psi$ and $\gamma\chi_{c1,c2}$. By requiring $M_{\gamma h, J/\psi} < 3.49 \text{ GeV}/c^2$, most background from $\psi(2S) \rightarrow \gamma\chi_{c1,c2}$ is removed. The resultant plot, shown in Fig. 4, shows a clear η signal superimposed on background, mainly from $\psi(2S) \rightarrow \pi^0\pi^0 J/\psi$. A fit is made using a Breit-Wigner resonance convoluted with a mass resolution function for the η signal plus a polynomial background, where the width of the η is fixed to its Particle Data Group (PDG) value [15] and the background function is determined from $\psi(2S) \rightarrow \pi^0\pi^0 J/\psi$ Monte Carlo simulated events that satisfy the same criteria as the data. The fit yields $N_{e^+e^-}^\eta = 2465 \pm 101$ for the $\gamma\gamma e^+e^-$ state and $N_{\mu^+\mu^-}^\eta = 3290 \pm 148$ for the $\gamma\gamma\mu^+\mu^-$ state. The fitted values of the η mass are $547.6 \pm 0.1 \text{ MeV}/c^2$ for the $\gamma\gamma e^+e^-$ channel and $547.7 \pm 0.1 \text{ MeV}/c^2$ for the $\gamma\gamma\mu^+\mu^-$ channel, consistent with the PDG value within 2σ .

A fit using a fourth-order background polynomial with parameters free is also performed to estimate the systematic error due to the background shape. This error is negligibly small.

D. Selection of $\psi(2S) \rightarrow \gamma\chi_{c1,c2}$

The processes $\psi(2S) \rightarrow \pi^0 J/\psi$, $\eta J/\psi$, and $\pi^0\pi^0 J/\psi$ contribute to the background for this channel. By requiring $M_{\gamma\gamma} < 0.53 \text{ GeV}/c^2$, most of the background from $\psi(2S) \rightarrow \eta J/\psi$ and a significant portion from $\psi(2S) \rightarrow \pi^0\pi^0 J/\psi$ are rejected. Fig. 5 shows the $M_{\gamma h, J/\psi}$ distribution for candidate $\psi(2S) \rightarrow \gamma\chi_{c1,c2}$ events. The remaining background is mainly due to $\psi(2S) \rightarrow \pi^0\pi^0 J/\psi$. The contribution from $\psi(2S) \rightarrow \pi^0 J/\psi$ is negligible due to its tiny branching fraction. Fig. 6 shows the $M_{\gamma h, J/\psi}$ distribution for

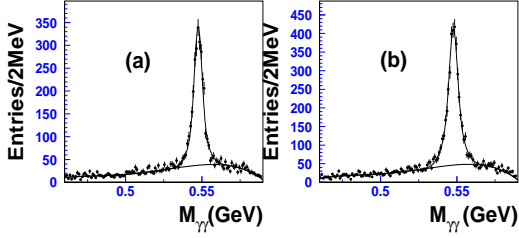


FIG. 4: Two photon invariant mass distribution for candidate $\psi(2S) \rightarrow \eta J/\psi$ events for (a) $\gamma\gamma e^+e^-$ and (b) $\gamma\gamma\mu^+\mu^-$.

$\psi(2S) \rightarrow \pi^0\pi^0 J/\psi$ Monte Carlo simulated events before and after the $M_{\gamma\gamma} < 0.53 \text{ GeV}/c^2$ requirement, the latter one is taken as the background shape in the fit. Two Breit-Wigner resonances convoluted with mass resolution functions plus a background function are fitted to the data. The widths for the $\chi_{c1,2}$ are fixed to the PDG values, and the mass resolution functions are determined by Monte Carlo simulation. The fit yields:

$$N_{e^+e^-}^{\chi_{c1}} = 5263 \pm 124, N_{e^+e^-}^{\chi_{c2}} = 2512 \pm 82,$$

$$N_{\mu^+\mu^-}^{\chi_{c1}} = 6752 \pm 178, N_{\mu^+\mu^-}^{\chi_{c2}} = 3358 \pm 96,$$

with the fitted masses of χ_{c1} and χ_{c2} equal to $3510.9 \pm 1.0 \text{ MeV}/c^2$ and $3555.9 \pm 1.0 \text{ MeV}/c^2$, respectively, consistent with the PDG values.

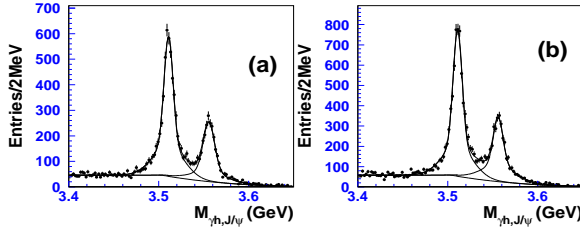


FIG. 5: Invariant mass $M_{\gamma h, J/\psi}$ distribution for candidate $\psi(2S) \rightarrow \gamma\chi_{c1,c2}$ events for (a) $\gamma\gamma e^+e^-$ and (b) $\gamma\gamma\mu^+\mu^-$.

IV. BRANCHING FRACTION DETERMINATION

For $\psi(2S) \rightarrow X$, the branching fraction is determined from

$$B(\psi(2S) \rightarrow X) = \frac{n^{obs}(\psi(2S) \rightarrow X \rightarrow Y)}{N_{\psi(2S)} \cdot B(X \rightarrow Y) \cdot \epsilon(\psi(2S) \rightarrow X \rightarrow Y)},$$

where Y stands for the final state, X the intermediate state, and ϵ the detection efficiency. The branching fraction of $X \rightarrow Y$ is taken from the PDG.

A. Detection efficiency

The detection efficiency is the product of the trigger efficiency ϵ_{trg} and the reconstruction-selection efficiency ϵ_{rs} . For the BES detector, the trigger efficiency for hadronic events is 1.000 ± 0.005 [16]. The reconstruction-selection efficiency is determined by Monte Carlo simulation. For the signal channels studied, generators taking into account phase space, angular distributions, and final state radiation are used for the event simulations. For the channel $\psi(2S) \rightarrow \pi^0\pi^0 J/\psi$, the common background for all signals, we use a generator, which gives the correct dipion mass and angular distributions [17].

For each of the channels analyzed, 50,000 Monte Carlo events are subjected to the same reconstruction and event selection as used for the data to determine the detection efficiencies, which are listed in Table III.

B. Efficiency corrections and systematic errors

Because the Monte Carlo is imperfect, it is necessary to correct the detection efficiencies obtained from simulations for the differences between the Monte Carlo simulation and the data. Differences come from the efficiencies of MDC tracking, particle identification, photon identification, and kinematic fitting. In addition, the uncertainties of the background shapes (estimated in Section 3), the number of $\psi(2S)$ events, and the branching fractions of the intermediate states also contribute to the final systematic error.

To investigate the difference in the lepton track efficiencies of the Monte Carlo simulation and the data, the lepton pair sample from the decay $\psi(2S) \rightarrow \pi^+\pi^- J/\psi, J/\psi \rightarrow l^+l^-$, which closely simulates the behavior of the lepton pair in the channels under study, is used. This study finds the tracking efficiency

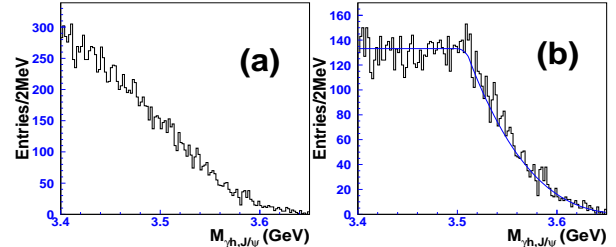


FIG. 6: Invariant mass $M_{\gamma h, J/\psi}$ distribution for Monte Carlo simulated $\psi(2S) \rightarrow \pi^0\pi^0 J/\psi$ events ($\gamma\gamma\mu^+\mu^-$ final state). (a) Before the $M_{\gamma\gamma} < 0.53 \text{ GeV}/c^2$ requirement. (b) After the $M_{\gamma\gamma} < 0.53 \text{ GeV}/c^2$ requirement.

correction factor is 1.012 ± 0.009 for e^+e^- pairs and 1.002 ± 0.008 for $\mu^+\mu^-$ pairs. For charged particle identification, S is used to separate e^+e^- and $\mu^+\mu^-$ pairs. The same lepton pair sample is used to determine the particle identification efficiency difference between Monte Carlo simulation and data by determining efficiencies for each with and without this particle identification requirement. The correction factor is found to be 0.951 ± 0.008 for e^+e^- pairs and 0.972 ± 0.006 for $\mu^+\mu^-$ pairs.

For the photon selection used, studies show that the efficiency difference between data and Monte Carlo is 2% for each photon [18]. We take this difference as the systematic error in photon selection, and no correction to the efficiency is made. In addition, the rib in the BSC causes an inefficiency in photon detection. The systematic error due to the rib efficiency, listed in table I, is obtained by comparing results with photons in the rib region removed with those when they are not removed.

The systematic error due to kinematic fitting comes from the differences between data and Monte Carlo simulation in the measurements of track momentum, the track fitting error matrix, and the photon energy and direction. For the charged track part, the difference is estimated using the $\psi(2S) \rightarrow \pi^+\pi^- J/\psi$, $J/\psi \rightarrow l^+l^-$ sample. For the photon part, a careful calibration of the neutral cluster information in the BSC is performed and the difference with and without the calibration applied to both the data and Monte Carlo is used to determine the systematic error in this part [19].

Table I summarizes the efficiency correction factors and uncertainties from all sources, while Table II lists the systematic errors for the channels under study. The branching fractions and corresponding errors for all intermediate state decays are taken from the PDG [20].

C. Results and discussion

Using the fitting results and the efficiencies and correction factors for each channel, we determine the branching fractions listed in Table III. We also obtain the product branching fractions

$$B(\psi(2S) \rightarrow \gamma\chi_{c1}) \cdot B(\chi_{c1} \rightarrow \gamma J/\psi) = (2.81 \pm 0.05 \pm 0.23)\%,$$

$$B(\psi(2S) \rightarrow \gamma\chi_{c2}) \cdot B(\chi_{c2} \rightarrow \gamma J/\psi) = (1.62 \pm 0.04 \pm 0.12)\%.$$

Our $B(\psi(2S) \rightarrow \pi^0 J/\psi)$ measurement has improved precision by more than a factor of two compared with other experiments, and the BES $\psi(2S) \rightarrow \eta J/\psi$ branching fraction is the most accurate single measurement. Our $B(\psi(2S) \rightarrow \pi^0 J/\psi)$ agrees better with the Mark-II result [5] than with the Crystal Ball result [6], while $B(\psi(2S) \rightarrow \gamma\chi_{c1,c2})$ agrees well with

the Crystal Ball results [6]. Much of the systematic error on $B(\psi(2S) \rightarrow \gamma\chi_{c1,c2})$ comes from the uncertainties on $B(\chi_{c1} \rightarrow \gamma J/\psi)$ and $B(\chi_{c2} \rightarrow \gamma J/\psi)$.

Using Partially Conserved Axial-vector Currents (PCAC), Miller *et al* [8] predicts:

$$R = \frac{\Gamma(\psi(2S) \rightarrow \pi^0 J/\psi)}{\Gamma(\psi(2S) \rightarrow \eta J/\psi)} = \frac{27}{16} \left(\frac{p_\pi}{p_\eta} \right)^3 r^2, \quad (1)$$

where $r = (m_d - m_u)/(m_s - 0.5 \cdot (m_d + m_u))$ and p_π and p_η are the π and η momenta in the $\psi(2S)$ rest frame. With the conventionally accepted values of $m_s = 150$ MeV/c², $m_d = 7.5$ MeV/c², $m_u = 4.2$ MeV/c² given by Weinberg [21], the ratio R equals 0.0162, which is smaller than our measurement (0.048 ± 0.005) [22] by a factor of three. Based on an effective Lagrangian approach, Casalbuoni *et al* [9] obtain an improved expression

$$R = \frac{27}{16} \left(\frac{p_\pi}{p_\eta} \right)^3 r^2 \left[\frac{1 + \frac{2B}{3A} \frac{\hat{\lambda} f_\pi}{m_{\eta'}^2 - m_{\pi^0}^2}}{1 + \frac{B}{A} \frac{\hat{\lambda} f_\pi}{m_{\eta'}^2 - m_\eta^2}} \right]^2, \quad (2)$$

in which $\hat{\lambda}$ characterizes the η - η' mixing, B/A is a not yet determined parameter in the effective Lagrangian. $f_\pi = (130 \pm 5)$ MeV is obtained from PDG. Using the approximation [23]

$$\hat{\lambda} = \sqrt{\frac{3}{2}} \left(\frac{m_{\eta'}^2 - m_\eta^2}{m_s - \frac{m_u + m_d}{2}} \right) \tan \theta_P, \quad (3)$$

where $\theta_P \approx -20^\circ$ [15] is the η - η' mixing angle, we obtain $\hat{\lambda} \approx 1.91$ GeV. With our measured value of R , we infer the parameter $\frac{B}{A}$ equals -1.42 ± 0.12 or -3.11 ± 0.15 in Equation (2).

In terms of QCD multipole expansion, Kuang *et al* [11] predict the ratio

$$R' \approx \left(\frac{m_c}{m_b} \right)^2 \cdot \left(\frac{p_\eta(\Upsilon')}{p_\eta(\psi(2S))} \right)^3 \cdot \left(\frac{f(\Upsilon')}{f(\psi(2S))} \right)^2, \quad (4)$$

$$R'' \approx \left(\frac{m_c}{m_b} \right)^2 \cdot \left(\frac{p_\eta(\Upsilon'')}{p_\eta(\psi(2S))} \right)^3 \cdot \left(\frac{f(\Upsilon'')}{f(\psi(2S))} \right)^2, \quad (5)$$

where $f(\psi(2S))$, $f(\Upsilon')$, and $f(\Upsilon'')$ are the transition amplitudes of $\psi(2S) \rightarrow J/\psi \pi \pi$, $\Upsilon' \rightarrow \Upsilon \pi \pi$, and $\Upsilon'' \rightarrow \Upsilon \pi \pi$, respectively, which depend on the potential model describing the heavy quarkonia. Taking the QCD motivated Buchmüller-Grunberg-Tye potential [24] as an example, the predicted values are $R'_{BGT} = 0.0025$ and $R''_{BGT} = 0.0013$. With our measurements of $B(\psi(2S) \rightarrow \eta J/\psi)$ and PDG values of $\Gamma(\psi(2S))$, $\Gamma(\Upsilon' \rightarrow \Upsilon \eta)$ and $\Gamma(\Upsilon'' \rightarrow \Upsilon \eta)$, we obtain $R'_{exp} < 0.0098$ and $R''_{exp} < 0.0065$, which are consistent with the predictions of Equations (4) and (5).

The BES collaboration acknowledges the staff of BEPC for their hard efforts. The authors also thank Prof. Y. P. Kuang for enlightening discussions. This

TABLE I: Efficiency correction factors.

Channel	$\pi^0 J/\psi$		$\eta J/\psi$	
Final state	$\gamma\gamma e^+e^-$	$\gamma\gamma\mu^+\mu^-$	$\gamma\gamma e^+e^-$	$\gamma\gamma\mu^+\mu^-$
Track selection	1.012 ± 0.009	1.002 ± 0.008	1.012 ± 0.009	1.002 ± 0.008
Particle ID	0.951 ± 0.008	0.972 ± 0.006	0.951 ± 0.008	0.972 ± 0.006
5-C fit	1.000 ± 0.014	1.00 ± 0.02	1.000 ± 0.016	1.000 ± 0.038
γ efficiency	1.00 ± 0.04	1.00 ± 0.04	1.00 ± 0.04	1.00 ± 0.04
BSC rib	1.000 ± 0.023	1.000 ± 0.034	1.000 ± 0.031	1.000 ± 0.036
Total correction	0.962 ± 0.050	0.974 ± 0.057	0.962 ± 0.055	0.974 ± 0.067
Channel	$\gamma\chi_{c1}$		$\gamma\chi_{c2}$	
Final state	$\gamma\gamma e^+e^-$	$\gamma\gamma\mu^+\mu^-$	$\gamma\gamma e^+e^-$	$\gamma\gamma\mu^+\mu^-$
Track selection	1.012 ± 0.009	1.002 ± 0.008	1.012 ± 0.009	1.002 ± 0.008
Particle ID	0.951 ± 0.008	0.972 ± 0.006	0.951 ± 0.008	0.972 ± 0.006
5-C fit	1.000 ± 0.015	1.000 ± 0.049	1.000 ± 0.018	1.00 ± 0.052
γ efficiency	1.00 ± 0.04	1.00 ± 0.04	1.00 ± 0.04	1.00 ± 0.04
BSC rib	1.000 ± 0.043	1.000 ± 0.040	1.000 ± 0.019	1.000 ± 0.024
Total correction	0.962 ± 0.061	0.974 ± 0.075	0.962 ± 0.049	0.974 ± 0.070

TABLE II: Systematic errors (%)

Channel	$\pi^0 J/\psi$		$\eta J/\psi$	
Final state	$\gamma\gamma e^+e^-$	$\gamma\gamma\mu^+\mu^-$	$\gamma\gamma e^+e^-$	$\gamma\gamma\mu^+\mu^-$
efficiency correction	6.3	5.9	5.7	6.9
Number of $\psi(2S)$ events	4	4	4	4
$\mathcal{B}(\pi^0, \eta \rightarrow \gamma\gamma)$	negligible	negligible	0.65	0.65
$\mathcal{B}(J/\psi \rightarrow e^+e^-, \mu^+\mu^-)$	1.7	1.7	1.7	1.7
background shape	5.1	4.3	negligible	negligible
Total systematic error (%)	9.20	8.50	7.20	8.18
Channel	$\gamma\chi_{c1}$		$\gamma\chi_{c2}$	
Final state	$\gamma\gamma e^+e^-$	$\gamma\gamma\mu^+\mu^-$	$\gamma\gamma e^+e^-$	$\gamma\gamma\mu^+\mu^-$
efficiency correction	6.3	7.7	5.1	7.2
Number of $\psi(2S)$ events	4	4	4	4
$\mathcal{B}(\chi_{cJ} \rightarrow \gamma J/\psi)$	8.5	8.5	8.9	8.9
$\mathcal{B}(J/\psi \rightarrow e^+e^-, \mu^+\mu^-)$	1.7	1.7	1.7	1.7
Total systematic error (%)	11.44	12.26	11.14	12.25

TABLE III: Results. Note that much of the systematic error on $B(\psi(2S) \rightarrow \gamma\chi_{c1,c2})$ is due to the uncertainty on $B(\chi_{c1,c2} \rightarrow \gamma J/\psi)$.

Channel	$\pi^0 J/\psi$		$\eta J/\psi$	
Final state	$\gamma\gamma e^+e^-$	$\gamma\gamma\mu^+\mu^-$	$\gamma\gamma e^+e^-$	$\gamma\gamma\mu^+\mu^-$
Number of events	123 ± 18	155 ± 20	2465 ± 101	3290 ± 148
Efficiency(%)	11.21	13.34	26.94	34.07
Sys. error (%)	9.68	8.77	8.54	8.40
Correction factor	0.962	0.974	0.962	0.974
BR (%)	$0.139 \pm 0.020 \pm 0.013$	$0.147 \pm 0.019 \pm 0.013$	$2.91 \pm 0.12 \pm 0.21$	$3.06 \pm 0.14 \pm 0.25$
Combine BR (%)	$0.143 \pm 0.014 \pm 0.013$		$2.98 \pm 0.09 \pm 0.23$	
PDG (%)	0.096 \pm 0.021		3.13 \pm 0.21	
Channel	$\gamma\chi_{c1}$		$\gamma\chi_{c2}$	
Final state	$\gamma\gamma e^+e^-$	$\gamma\gamma\mu^+\mu^-$	$\gamma\gamma e^+e^-$	$\gamma\gamma\mu^+\mu^-$
Number of events	5263 ± 124	6752 ± 178	2512 ± 82	3358 ± 96
Efficiency(%)	23.88	29.24	19.70	25.54
Sys. error (%)	12.23	12.45	12.10	12.44
Correction factor	0.962	0.974	0.962	0.974
BR (%)	$8.73 \pm 0.21 \pm 1.00$	$9.11 \pm 0.24 \pm 1.12$	$7.90 \pm 0.26 \pm 0.88$	$8.12 \pm 0.23 \pm 0.99$
Combine BR (%)	$8.90 \pm 0.16 \pm 1.05$		$8.02 \pm 0.17 \pm 0.94$	
PDG (%)	8.4 \pm 0.6		6.4 \pm 0.6	

work is supported in part by the National Natural Science Foundation of China under contracts Nos. 19991480, 10225524, 10225525, the Chinese Academy of Sciences under contract No. KJ 95T-03, the 100 Talents Program of CAS under Contract Nos. U-11, U-24, U-25, and the Knowledge Innovation Project

of CAS under Contract Nos. U-602, U-34 (IHEP); by the National Natural Science Foundation of China under Contract No. 10175060 (USTC); and by the Department of Energy under Contract No. DE-FG03-94ER40833 (U Hawaii).

-
- [1] W. M. Tanenbaum et al., Phys. Rev. Lett. **36**, 402 (1976).
 - [2] C. J. Biddick et al., Phys. Rev. Lett. **38**, 1324 (1977).
 - [3] W. Bartel et al., Phys. Lett. **B79**, 492 (1978).
 - [4] R. Brandelik et al., Nucl. Phys. **B160**, 426 (1979).
 - [5] T. Himel et al., Phys. Rev. Lett. **44**, 920 (1980).
 - [6] M. J. Oreglia et al., Phys. Rev. Lett. **45**, 959 (1980); J. Gaiser et al., Phys. Rev. **D34**, 711 (1986).
 - [7] B. L. Ioffe and M. A. Shifman, Phys. Lett. **B95**, 99 (1980).
 - [8] G. A. Miller et al., Phys. Rep. **194**, 1 (1990).
 - [9] R. Casalbuoni *et al* Phys. Lett. B309,163(1993).
 - [10] T. M. Yan, Phys. Rev. **D22**, 1652 (1980).
 - [11] Y.P.Kuang and T.M.Yan Phys. Rev. D24,2874(1981); Y.P.Kuang *et al* Phys. Rev. D37,1210(1988).
 - [12] J. Z. Bai et al., BES Collab., Nucl. Instr. Meth. **A344**, 319 (1994).
 - [13] J. Z. Bai et al., BES Collab., Nucl. Instr. Meth. **A458**, 627 (2001).
 - [14] X. H. Mo et al., accepted to HEP & NP.
 - [15] Particle Data Group, K. Hagiwara et al., Phys. Rev. **D66**, 010001 (2002).
 - [16] J. Z. Bai et al., BES Collab., Phys. Rev. Lett. **84**, 594 (2000).
 - [17] J. Z. Bai et al., BES Collab., Phys. Rev. **D62**, 032002 (2000).
 - [18] J. Z. Bai et al., BES Collab., submitted to Phys. Rev. D, hep-ex/0402013.
 - [19] J. Z. Bai et al., BES Collab., Phys. Rev. **D67**, 112001 (2003).
 - [20] The branching fractions for $\chi_{c1,2} \rightarrow \gamma J/\psi$ are quoted from the 2003 WWW update of the Review of Particle Physics (<http://pdg.lbl.gov/2003/mxxx.html>).
 - [21] S. Weinberg, "The problem of mass", in a Festschrift for I. I. Rabi, ed. L. Motz (New York Academy of Sciences, New York, 1978).
 - [22] Part of the systematic error cancels in the calculation of R .
 - [23] Y.P.Kuang, private Communications; see also CERN Yellow Report on *Quarkonium Physics* (to be published).
 - [24] W.Buchmüller *et al.* Phys. Rev. Lett.45,103(1980); W.Buchmüller *et al.* Phys. Rev. D24,132(1981).